

## Experimental Investigation of Nonlinear Dynamics in the Fermilab Tevatron

A. Chao, D. Johnson, S. Peggs, J. Peterson, C. Saltmarsh, and L. Schachinger  
*Superconducting Supercollider Central Design Group, Berkeley, California 94720*

R. Meller, R. Siemann, and R. Talman  
*Newman Laboratory of Nuclear Studies, Cornell University, Ithaca, New York 14853*

P. Morton  
*Stanford Linear Accelerator Center, Stanford, California 94305*

D. Edwards, D. Finley, R. Gerig, N. Gelfand, M. Harrison, R. Johnson, N. Merminga, and M. Syphers  
*Fermi National Accelerator Laboratory, Batavia, Illinois 60510*

(Received 11 July 1988)

The nonlinear dynamics of transverse particle oscillations in the Fermilab Tevatron is studied experimentally and compared with prediction. Accurate measurements of various phase-space features are obtained. A theoretically expected metastable state of the accelerator, with particles captured on nonlinear resonance islands, is demonstrated experimentally, and stability of the state is investigated.

PACS numbers: 41.80.Gg, 03.20.+i, 05.45.+b, 29.20.Dh

This Letter describes a beam-dynamics experiment, performed in the Fermilab Tevatron, that was largely motivated by planning for the Superconducting Supercollider. In intentionally adding nonlinear elements in order to “mock up” some nonlinear features anticipated for the Superconducting Supercollider, observations were made which are applicable to areas of physics much broader than accelerator physics, as they relate to the phase-space description of nonlinear oscillations. Those features are described here. The subject of this Letter, then, is the experimental study of a Hamiltonian system and its Poincaré map, a century-old entity with value previously restricted to theory.

For this experiment the Tevatron can be regarded as a linear system on which nonlinearity in the form of sixteen sextupole magnets, each of strength  $S$ , was intentionally superimposed. The experimental procedure starts with a “needle beam” consisting of some  $10^{10}$  circulating stored protons, all assumed, for now, to have essentially the same momentum and to be on the central orbit. Next the same angular deflection  $D$  is impulsively applied to every particle by a pulsed deflecting magnet. The subsequent beam-centroid displacement is sensed electrically for as many as a million accelerator turns by beam-position monitors (BPM). These measurements are used to generate an experimental Poincaré plot, an object described in the following theoretical discussion.

To an excellent approximation, the equation of motion satisfied by  $x(s)$ , the horizontal particle deviation from the central orbit, is

$$d^2x/ds^2 + K(s)x = -\epsilon(s)x^2. \quad (1)$$

Here  $s$  is the longitudinal particle coordinate, which advances from 0 to  $C$ , the circumference, as the particle

completes one revolution of the accelerator. Particles execute “betatron” oscillations with linear focusing being due to quadrupole fields of strength  $K(s)$ . The number of oscillation periods in one revolution is called the tune: about 19.4 for the Tevatron. The anharmonic term in (1) is due to sextupole fields of strength  $\epsilon(s)$ , proportional to  $S$ . Both  $K(s)$  and  $\epsilon(s)$  are periodic functions of  $s$  with period  $C$ . The absence of damping in (1) is valid as the quality factor of these oscillations has a very high value  $> 10^9$ , making this a truly Hamiltonian system.

The concept of phase space is theoretically helpful and experimentally essential when analyzing these oscillations. In this description the coordinate  $x$  and the slope  $p \equiv dx/ds$  are treated on equal footing as dependent variables. By plotting their values  $x_t$  and  $p_t$  for successive passages,  $t=0,1,\dots$ , of the particle past a reference point in the accelerator, one obtains a “Poincaré surface of section.” After judicious choice of scales these points are given by  $x_t = a_t \cos \psi_t$  and  $p_t = -a_t \sin \psi_t$ , where  $a_t^2/2$  and  $\psi_t \approx 2\pi \nu t$  are “action-angle” variables. Time  $t$  is measured in units in which the revolution period is 1; in these units the frequency,  $\nu$ , is called the “fractional tune.” When the amplitude  $a_t$  is sufficiently small, it does not deviate from its average value  $a$ , and the phase-space point moves on a circle on the  $x$ - $p$  plot; any deviation is due to  $\epsilon(s)$ . Implicit in the restriction to the single Poincaré plane is complete ignorance of the motion elsewhere in the ring. In particular, the number of complete cycles, and hence the integer part of the previously defined tune, are undetectable. The terms phase-space plot and Poincaré plot are used interchangeably from this point on.

Hamiltonian concepts are important in analyzing phase-space motion. The Hamiltonian leading to (1) is

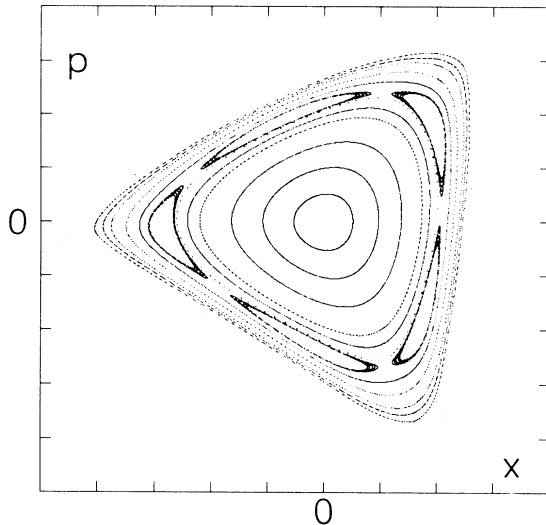


FIG. 1. Poincaré map generated by numerically tracking particles of various amplitudes. Most of the features have been demonstrated and measured.

$H(x, p, s) = (p^2 + x^2)/2 + \epsilon(s)x^3/3$ . Here a Folquet transformation has been made, in order to replace the  $s$ -dependent factor  $K(s)$  by 1, to make  $H$  independent of  $s$  for small  $\epsilon$ . At sufficiently small amplitudes  $H$  is independent of  $s$ , making it a constant of the motion. This is equivalent to the  $a_t = a$  solution, since  $H$  and  $a^2 = x^2 + p^2$  are equivalent constants of the motion. Below, we will use the result that  $a$  is an "adiabatic invariant" which remains approximately constant when a parameter, such as  $K(s)$ , is slowly varied.

The expected phase-space structure is illustrated in Fig. 1. It was calculated by symplectic numerical tracking<sup>1</sup> through a representation of the lattice consisting of static elements, linear except for "chromaticity compensating sextupoles," and the sixteen main sextupoles. The former were calculated to be negligible, except with  $S=0$ . This was confirmed experimentally, and for most other calculations, for greater speed, only the sixteen main sextupoles were included. Nonlinear-error multipoles in the Tevatron, though known, and known to smaller yet, were not included.

Experimental investigation of this structure, starting at small amplitudes and working out, will now be described. The amplitude  $a$  is adjusted by means of the deflector strength  $D$ . Transverse displacements  $x_{1t}$  and  $x_{2t}$ , measured at two positions separated by about one quarter of a betatron wavelength, can be used to make a "raw" Poincaré plot, as will be shown below. The quantity  $p_t$  has to be obtained indirectly from these values and then  $a_t$  is calculated. Figure 2 shows a typical record of measured values of  $a_t$  for the first 500 turns after the beam has been deflected.

Values of  $\nu$  measured by fitting the early turns of data like those in Fig. 2 are plotted in Fig. 3; they agree well

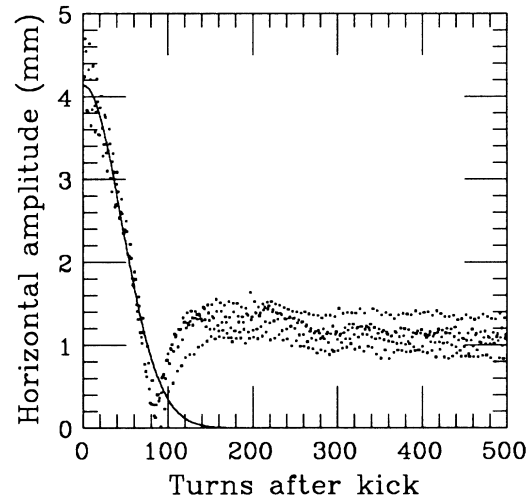


FIG. 2. Raw BPM turn-by-turn output for 500 turns after transverse deflection of the beam. The smooth fit has the theoretically expected Gaussian shape.

with calculations. The damping of centroid motion observed in Fig. 2, which appears to contradict the high quality factor of individual particle oscillations mentioned above, can now be understood. Because of the dependence  $\nu(a)$  of tune on amplitude, due to the anharmonic term of (1), different particles have slightly different tunes. Though the amplitudes start out in phase, they gradually lose coherence. Since the BPM measures the centroid of the full set of protons there is an apparent damping. Calculations of the decoherence, starting with the known beam dimensions, agree well with measured values. The persistent signal (not normally present), due to particle capture onto stable islands, is discussed below. The dip is due to destructive interference.

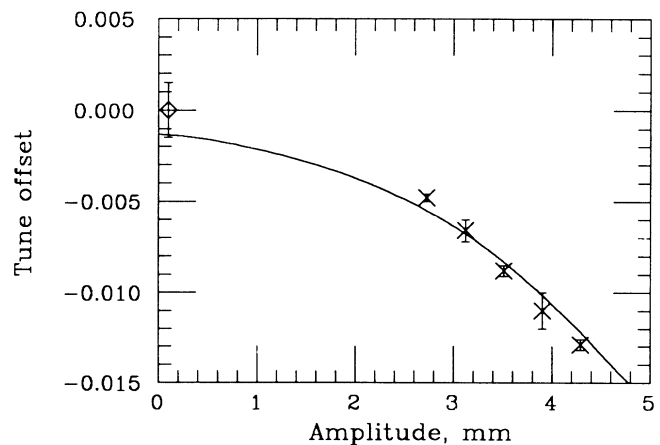


FIG. 3. Dependence of tune on amplitude. Data points are measured; the curve is predicted.

Next we consider the qualitative phase-space behavior as the amplitude is increased further out of the “linear” region. Deviation from circularity in Fig. 1, due to the  $s$ -dependent nonlinearities, can still be treated perturbatively. The distortion is quantified by the “smear” parameter, the fractional root mean square deviation of  $a$ . Quantitative comparison between observed and calculated smear is contained in Fig. 4, which again shows excellent agreement. Though the Hamiltonian  $H$ , being explicitly  $s$ -dependent, is no longer a constant of the motion, the phase-space points still lie on a smooth curve in this region, at least to the accuracy of the plot. The existence of such “regular” curves, of the form  $H_P(x,p) = \text{const}$ , is consistent with the so-called Kolmogorov-Arnol’d-Moser theory.<sup>2</sup>

At large amplitudes the regularity is lost and the motion is chaotic. This is shown on the periphery of Fig. 1. The largest regular contour is sometimes called the “dynamic aperture” of the accelerator. By intentionally “heating” the beam its transverse size was gradually enlarged until particles were lost. With use of a “flying wire” technique, the beam size was then measured to obtain the dynamic aperture. The measured aperture was approximately 20% less than the calculated aperture. We ascribe this to presently not understood effects which, on the millions-of-turns time scale on which the measurement was made, were not included in the hundreds-of-turns tracking calculations.

Finally, we have observed the chain of five “islands” of Fig. 1. The concept of resonance enters as follows. With the base tune (the tune with  $\epsilon = 0$ ) just above  $\frac{2}{5}$ , after 5 turns around the accelerator a particle returns close to where it started. The effect of the nonlinearity is to make the tune decrease with increasing amplitude (Fig. 3), and so there is one amplitude,  $a_R$ , for which the tune is exactly  $\frac{2}{5}$ , and the repetition is perfect. Furthermore, there is a frequency entrainment effect causing all near-

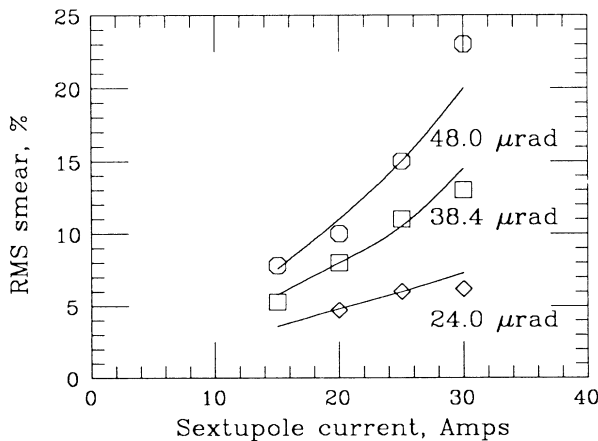


FIG. 4. Plot of smear vs  $S$  for various values of  $D$ . Data points are measured values; curves are predictions.

by amplitudes to “lock on” to exactly the same tune of  $\frac{2}{5}$ . This accounts for the islands. Their centers are called stable fixed points since a particle starting near one stays near forever. “Stroboscopically” viewing every fifth turn, the particle moves steadily along a regular oval curve, circulating around the fixed point in much the same way that a small-amplitude particle circulates around the origin. An island tune  $\nu_I$  is defined as the average number of revolutions around the island per turn around the accelerator.

The topology of Fig. 1 also requires five unstable fixed points between the islands. Some chaotic motion is inescapable in their vicinity, but that behavior is restricted to too small a phase-space area to have influenced our observations.

It follows that the accelerator should be capable of operating as a “different” accelerator in which the particles circulate indefinitely, not around the origin, but around the newly understood fixed points. This could be called an “excited state” of the accelerator, or, perhaps better, a metastable state, since the system is observed to “decay” with a lifetime as treat as a minute. The decay mechanism is not understood. Language has intentionally been employed to motivate observations similar to those made in the study of atomic systems. These observations include demonstrating the existence of the state, measuring its production probability and decay rate, and investigating its dependence on external variables.

Some of the protons are captured on the stable islands when a properly adjusted deflection is administered to the beam, with the sextupoles turned on to give resonant islands. This manifests itself by the *absence* of decoherence. All particles on one of these islands exhibit a tune

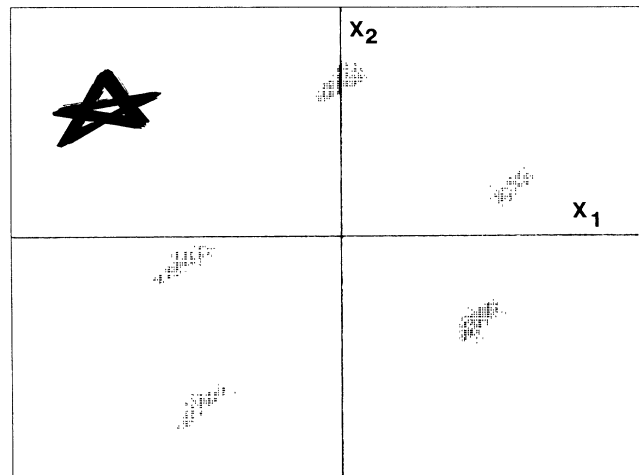


FIG. 5. “Raw experimental Poincaré map” exhibiting a metastable state of the accelerator. The “logo” in the corner of the plot is a demagnified view of the same data with successive points joined by straight lines. The point lands only on every second island, confirming the  $\frac{2}{5}$  identification.

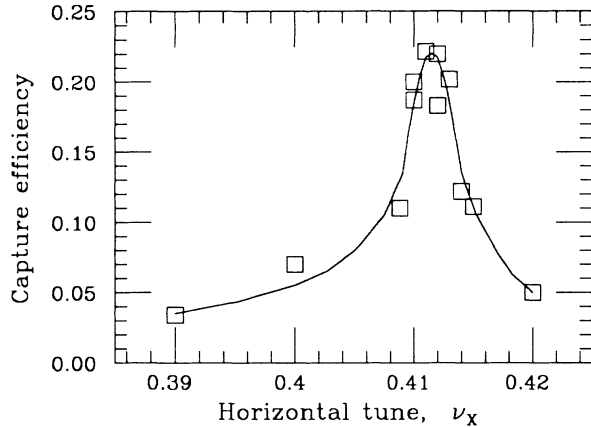


FIG. 6. Capture fraction measured as the island amplitude is moved through the deflection amplitude, by varying the base tune. The curve only guides the eye.

of exactly  $\frac{2}{5}$ , totally defeating the decoherence. This accounts for the signal persisting after a few hundred turns in Fig. 2. Signals like this have been observed to persist for over a minute (approaching a million turns). Spectral analysis yields a value  $\nu = 0.400\,010 \pm 0.000\,005$ , consistent with  $\frac{2}{5}$ . Figure 5 shows a thousand turns of data,  $x_1$  vs  $x_2$ , taken some seconds after the kick time. The five islands are clearly visible. Particle trapping was also observed at tunes of  $\frac{3}{7}$ ,  $\frac{3}{8}$ , and  $\frac{5}{13}$ .

To quantify the production probability, the "capture efficiency" was defined as the fraction of nondecoherent charge surviving 500 turns, well after the decoherence of uncaptured particles, and before appreciable decay has occurred. It depends on the relaxation between  $a$  and  $a_R$ , on the relation between beam size and island size, and on the angular orientation in phase-space of the islands. Experimentally, with  $D$  (and hence  $a$ ) held fixed, the capture efficiency was measured as the base tune (and hence  $a_R$ ) was varied. A classical resonance response is shown in Fig. 6, with the capture efficiency

only being appreciable for  $a \approx a_R$ .

To investigate the decay mechanism for loss of particles out of the stable islands the decay rate was measured as the accelerator base tune was sinusoidally modulated with a tune range of  $\pm \Delta\nu$ , at a frequency (i.e., tune) of  $\nu_M$ . As  $\nu_M$  was increased at fixed  $\Delta\nu$ , the decay rate remained small, until a rather sharp break point was reached, beyond which the decay rate increased rapidly. The model of adiabatic behavior, due to Chao and Month,<sup>3</sup> has the resonant islands moving in phase space at a rate sufficiently slow that trapped particles remain trapped. The location of the break point, and the adiabatic condition  $\nu_M \Delta\nu < \nu_I^2/5$ , can be used to obtain an estimated value of 0.007 for  $\nu_I$ .<sup>4</sup>

Measurement of phase-space features with a precision not previously achieved, at least in the context of accelerator physics, has been described. We regard the island-capture results as preliminary but indicative of an interesting research direction. It is pleasing to see such a complicated device as a storage ring exhibiting such exotic, yet simply understandable, behavior. This should permit controlled investigations of long-term stability, of interest both for accelerators and for mechanical systems in general.

It is a pleasure to acknowledge the participation of our CERN colleagues, A. Hilaire and L. Vos, in the measurements reported here. The Superconducting Supercollider Central Design Group and Fermi National Accelerator Laboratory are operated by the Universities Research Association under Contract with the U.S. Department of Energy.

<sup>1</sup>L. Schachinger and R. Talman, *Part. Accel.* **22**, 35 (1987).

<sup>2</sup>V. I. Arnold, *Mathematical Methods of Classical Mechanics* (Springer-Verlag, Berlin, 1978).

<sup>3</sup>A. W. Chao and M. Month, *Nucl. Instrum. Methods* **121**, 129 (1974).

<sup>4</sup>S. Peggs, Superconducting Supercollider Central Design Group Report No. SSC-175, June, 1988 (unpublished).

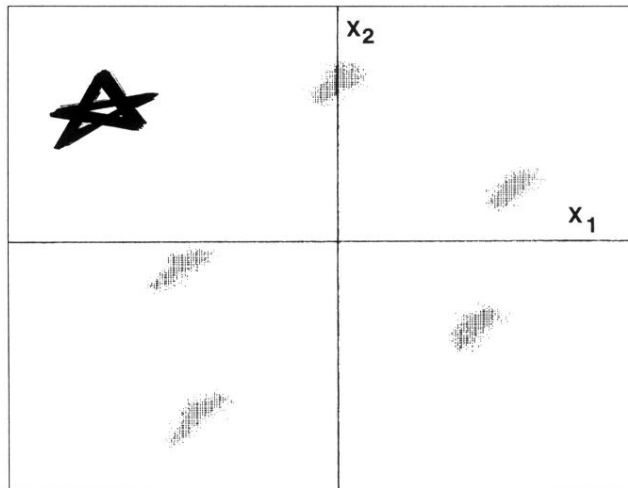


FIG. 5. “Raw experimental Poincaré map” exhibiting a metastable state of the accelerator. The “logo” in the corner of the plot is a demagnified view of the same data with successive points joined by straight lines. The point lands only on every second island, confirming the  $\frac{2}{5}$  identification.